Sustainable Energy & Fuels

ROYAL SOCIETY OF CHEMISTRY

PAPER

View Article Online
View Journal | View Issue

Cite this: *Sustainable Energy Fuels*, 2021, 5, 3895

Electrical conductivity of beech sawdust using graphite catalytic coating: unlocking the microwave-assisted thermolysis efficiency of lignocellulosic biomass†

Florent P. Bouxin, * Jiajun Fan, Vitaliy L. Budarin* and James H. Clark

The coating of the beech sawdust using a catalytic amount of graphite (as low as 0.25 wt%) allowed a step improvement in the microwave-assisted thermolysis. Results demonstrated that the pyrolysis performance was linked to an electrical conductivity threshold of the coated samples rather than a gradual increase. With as low as 0.13 mS m^{-1} of electrical conductivity, the 0.75 wt% graphite coated sawdust (250–500 μm) was efficiently gasified with up to 43 wt% of gas (30 wt% of carbon monoxide, 25 vol% of hydrogen). Initial particle size impacted the thermolysis performance where optimal size (250–500 μm) provided high heat homogeneity due to efficient graphite coating and low temperature gradient between the outer and inner part of the sawdust. The small initial particle size (75–250 μm) was unsuitable for microwave pyrolysis, exhibiting a too large surface area for efficient coating with 0.75 wt% of graphite which was confirmed by the absence of electrical conductivity (<0.003 mS m^{-1}). The electrical conductivity can be used as a marker to evaluate the suitability of the sample for microwave-assisted pyrolysis. Unlike simple graphite mixing, the mechanical coating allowed more than 20-fold decrease of susceptor quantity, providing more homogeneous samples with higher reproducibility.

Received 21st April 2021
Accepted 26th June 2021

DOI: 10.1039/d1se00610j

rsc.li/sustainable-energy

Introduction

Our growing consumption of fossil resource for the production of energy and chemicals is leading to the exponential increase of the greenhouse gas (GHG) emission, fuelling unprecedented climate change.[1] Looking for more sustainable ways to produce energy, fuel and chemicals is one of the biggest challenges of the 21st century.[2] Renewable energy sources such as wind, solar and hydroelectric have already been implemented as suitable and more sustainable alternatives to coal electricity.[3] Amongst the alternatives to fossil fuel, biomass is the only sustainable substitute that can provide both energy and bio-based chemicals.[4] The use of biomass as a substitute to petrol and coal have been commercially achieved in transportation (bioethanol)[5] and solvent (Cyrene)[6] or plastic (PLA, PBS)[7] sectors. The conversion of biomass to fuels and chemicals relies on the combination of three pathways (biological, chemical or thermal) which constitutes the pillars of the emerging biorefinery.[2] The thermochemical pathway for the biomass conversion accounts combustion, pyrolysis and gasification for the production of energy, bio-oil and syngas respectively. In 2018, the biomass gasification generated 1 GW output power and accounts several large-scale facilities in Skive, Denmark and Vaskiluodon Voima, Finland. However, this IEA report recently pointed out that the economic issue of the biomass gasification prevented the scale-up of many demonstration plants.[8] Another study reported that the biomass pyrolysis and gasification were challenged by the problem of tar production which leads to equipment blockage and costly maintenance.[3] As consequence, the challenge facing the conventional approach of biomass thermolysis could contribute to redesign of the whole process, fuelling research on new cutting-edge technology for biomass thermal conversion.

Microwave-assisted thermolysis of biomass is recently attracting much attention due to the ability of certain raw materials to produce heat from electromagnetic fields, allowing fast, uniform and volumetric heating.[9–12] Moreover, studies have shown that microwave pyrolysis of biomass generated less tar than the conventional pyrolysis.[13] The contactless energy transfer provides by the microwave technology is considered as green alternative to conventional and especially suited when fast heating rate is required (*e.g.* gasification).[14] Previous work reported that the hemicelluloses, cellulose and lignin contained within lignocellulosic biomass could be activated with MW irradiation at specific temperatures.[15] However, those work were performed in closed vessel,[16] relied on microwave active biomass (*e.g.* algae) or required high microwave power density.[10,17] In fact, most of the lignocellulosic biomass (*e.g.*

Green Chemistry Centre of Excellence, Department of Chemistry, University of York, York, YO10 5DD, UK. E-mail: florent.bouxin@york.ac.uk; vitaliy.budarin@york.ac.uk

† Electronic supplementary information (ESI) available. See DOI: 10.1039/d1se00610j

wood sawdust) exhibit low dielectric properties limiting direct microwave-assisted thermolysis.[10,18] Previous work reported that the pine sawdust has a loss tangent (δT) of 0.01 which is ten times lower than water ($\delta T = 0.11$) at 25 °C and 2.45 GHz.[18] To overcome its low microwave absorbing properties, the biomass is generally mixed with microwave susceptors such as biochar, activated carbon or silicon carbide.[19–21] In microwave-assisted thermolysis, most of the previous works used a fixed bed reactor where the biomass was dropped on preheated microwave absorbents such as silicon carbide (SiC) or carbonaceous material.[19,22,23] The heat transfer produced by conduction from the pre-heated microwave susceptor to the freshly dropped biomass could be closely assimilated conventional heating. In that case, any specific interaction between the microwave and the biomass was often ignored. Otherwise, the vast majority of the microwave-assisted gasification has been performed on biomass char in the presence of carbon dioxide or steam as oxidative reagent, high microwave absorbance properties of the biochar allowing the gasification to be done without the addition of microwave susceptors.[24,25] In the case of direct microwave-assisted thermolysis of the lignocellulosic biomass, microwave absorbing materials (metal, activated carbon, biochar) are often required to generate fast heating rate.[20,21] Recently, Liu *et al.* reported the production of hydrogen-rich syngas from lignocellulosic biomass using high MW absorbing property of less defective graphene aerogel.[26] The high syngas production was attributed to outstanding MW absorbance of the less defective graphene that could reach temperature above 1000 °C. Heating rate being of the critical parameters that provides efficient pyrolysis and gasification, proximity between the susceptor and the biomass is crucial and generally required large amount of susceptor (*e.g.* 20 wt% or above). In other word, large proportion of starting material won't directly contribute to the yield of bio-oil or biogas while taking a significant volume of the reactor. Other work reported that minimizing the amount of susceptor is essential for large-scale application as high susceptor to biomass ratio lead to higher energy consumption per unit of biomass.[27] Therefore, we postulated that instead of simply mixing large amount of susceptor with the biomass, the contact between the susceptors and the biomass could be greatly improved by the coating of the biomass with microwave absorbing materials. In order to provide microwave active coating, graphite was selected for its exfoliation ability. Mechano-assisted preparation of catalysts for various applications linked to conversion of biomass have recently been reviewed.[28] For example, mechano-assisted coating of cellulose with graphite for graphene preparation has already been reported.[29] Others also demonstrated that graphene was produced by graphite exfoliation using mechano-assisted procedure.[30,31]

To the best of our knowledge, there is no work reporting the microwave activation of woody biomass using graphite mechanical coating. In this study, graphite coated sawdust was produced using a mechano-assisted procedure which is solvent-free and less time-consuming than typical wet incipient impregnation.[28] The coated material was then submitted to microwave-assisted pyrolysis. We believe that mechanical coating of graphite to the woody biomass could provide better understanding on specific MW activation of biomass component during microwave-assisted thermolysis, unlocking greener technologies to convert renewable and abundant feedstock to key building blocks. Moreover, improving the microwave absorbance of the wood particle will allow higher energy efficiency of the microwave assisted pyrolysis, providing better opportunity for technology commercialisation.

Experimental

Materials

The beech sawdust was supplied from Norske Skoog, a paper industry company. The sawdust was sieved to a particle sizes ranged from 75–250, 250–500 and 500–1000 μm. Graphite powder 99% (<45 μm), HPLC-grade acetone was purchased from Sigma-Aldrich.

Sawdust compositional analysis

The water content in the sawdust was measured by drying the sawdust at 105 °C for 24 h. The ash content was measured after calcination of the dry sawdust at 625 °C in air for 4 h. The two-step acid hydrolysis was used to quantify the amount of cellulose (glucan), hemicelluloses (xylan, arabinan) and Klason lignin (acid-insoluble lignin) in the sawdust. Dry sawdust samples were soaked in 72 wt% H_2SO_4 for 2 h at 40 °C and then autoclaved at 121 °C in 4 wt% of H_2SO_4 for 1 h. The hydrolysate was analysed by HPLC, and the residue was filtered in a ceramic porous crucible (porosity 8 μm), washed with distillate water and dried at 105 °C. The acid-insoluble lignin was determined after calcination of the dry residue at 500 °C for 6 h.

Mechanical coating of the graphite to the beech sawdust

From 0 to 1.5 wt% of graphite was mixed with beech sawdust (500–1000 μm). The mixture was then ball milled using Retsch PM100 planetary ball mill. 11 g of the mixture was placed in 250 mL stainless steel jar containing 10 stainless steel balls (20 mm dia.) and the graphite coating was performed at 120 rpm with 10 min interval, reversal rotation, 30 s break and from 1 to 8 h. In this low-speed rotation condition, negligible internal heating (>40 °C) was recorded using thermometer inserted inside quickly after 8 h ball milling. For the graphite loading effect, coated sawdust with particle size above 75 μm obtained after 2 h ball milling was used for the pyrolysis/cracking experiments. To investigate the effect of ball milling duration, the 1 wt% coated sawdust were sieved after mechanical coating, and particle sizes ranging from 250 to 500 μm were used for the microwave-assisted pyrolysis/cracking. Finally, to measure the effect of the initial particle size of the beech sawdust, three sawdust fractions (75–250, 250–500 and 500–1000 μm) were ball milled in presence of 0.75 wt% of graphite following the same protocol as above and 2 h duration. On sample preparation without dry ball milling step, the raw beech sawdust (250–500 μm) was mixed with 5 or 10 wt% of graphite.

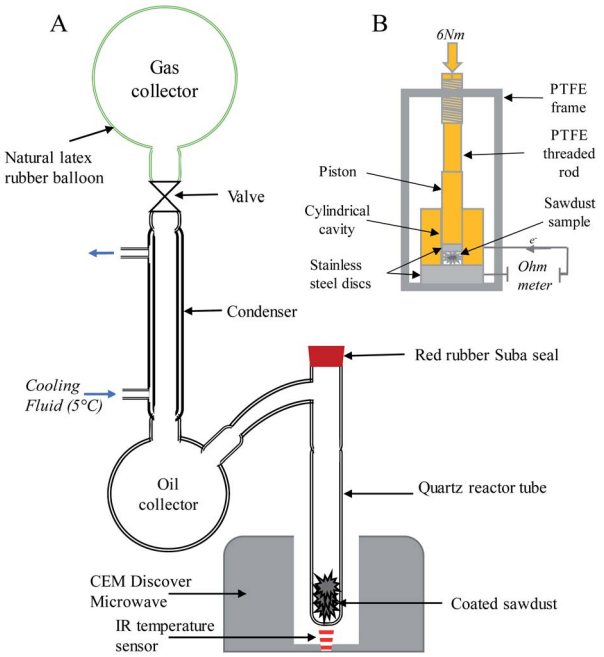

Fig. 1 (A) Set-up for microwave-assisted pyrolysis of graphite coated beech sawdust, (B) lab-made apparatus for measuring the coated sawdust electrical conductivity.

Microwave-assisted thermolysis

As illustrated in Fig. 1A, the microwave-assisted thermolysis was performed on the Discover SP microwave (CEM) at 2.45 GHz. Sawdust material (1 g) was placed in the quartz reactor tube. A 100 mL round bottom flask was placed between the reactor and the condenser (cooled at 5 °C) to facilitate the bio-oil recovery. On the top of the condenser was fitted a rubber balloon allowing the reaction to be conducted under inert atmosphere. Argon atmosphere was achieved by vacuuming the system at 40 mbar followed with argon addition from the prefilled rubber balloon. The procedure was repeated five times to ensure complete removal of air. The pyrolysis was performed at various microwave power and stopped once the temperature reached 300 °C. When the temperature did not reach 300 °C, the reaction was stopped after 5 min. After cooling, 100 mL of nitrogen was added to the system *via* the Suba seal as the internal standard for gases quantification and proper gases mixing was ensured by syringe pumping for at least five times. After gas sampling using inert multi-layer foils gas bag (SupelTM), the residue was filtered over a porous sintered crucible (8 μm), washed with acetone and dried at 60 °C for 48 h. The bio-oil was recovered from the collector, the residue and reactor walls using acetone. The acetone was evaporated under nitrogen blown to recover the bio-oil. Then, the ethanol was used to co-evaporate the water present in the bio-oil.

Bio-gas analysis

The bio-gas produced from the gasification of the beech sawdust were analysed by Carboxen 1010 PLOT capillary column (0.53 mm × 30 m) fitted to Agilent GC/TCD 7820a. Oven program temperature was hold at 80 °C for 1 min, increased at 25 °C min^{-1} to 250 °C and hold for 20 min. Injector and TCD detector were set at 200 °C and 250 °C, respectively. 0.5 mL of the gas mixture was injected and carried by argon at 3 mL min^{-1}. The TCD response was calibrated with pure gas mixtures (H_2, N_2, CO, CO_2, CH_4, CHCH, CH_2CH_2 and CH_3CH_3). Nitrogen was used as internal standard.

Electrical conductivity analysis of the sawdust

The electrical conductivity of the coated sawdust was measured using lab-made apparatus. As illustrated in Fig. 1B, 1 g of coated or uncoated beech sawdust was introduced in the cylindrical cavity on the top of 15 mm diameter stainless steel disc. A piston with 15 mm diameter stainless steel disc was placed over the sawdust to pack the biomass. A PTFE mounted frame from milestone Flexiwave vessel was used in order to apply pressure using a threaded PTFE rod. The constant pressure was applied on the packed coated sawdust using Norbar adjustable torque wrench at 6 N m. As illustrated eqn (1), the resistivity of the material (ρ) was measured using the resistance (R) of the material, the surface area (S.A) of the disc and the length (L) of the packed biomass. Then, the conductivity (σ) can be calculated as shown in eqn (2)

$$\text{Resistivity } (\rho) = \frac{R \times \text{S.A}}{L} \quad (1)$$

$$\text{Conductivity } (\sigma) = \frac{1}{(\rho)} \quad (2)$$

Karl–Fisher analysis

The water content of the acetone extract was measured by Karl–Fisher technique (907 Titrando Metrohm autotitrator). Hydranal Composite 5K and Hydranal KetoSolver were used as the titrant and working medium, respectively. Analysis of at least 120 s duration with a polarising current of 50 μA, stop voltage of 250 mV and drift point criterion of <20 μL min^{-1} was performed at ambient temperature under vigorous stirring. Acetone blank was also analysed to substrate the moisture from the solvent.

Thermal gravimetric analysis

The thermal decomposition of the coated or uncoated sawdust was performed on simultaneous thermal analyser STA625 (Stanton Redcroft). Ten mg of sample was pyrolysed under nitrogen flow (60 mL min^{-1}) from room temperature to 625 °C at 10 °C min^{-1}.

Scanning electron microscopy

Scanning Electron Microscopy (SEM) images were taken on a JEOL JSM-6490LV operating in high vacuum mode at 5 kV, using a tungsten filament and secondary electron detector to determine the morphology and structure of the graphite coated sawdust. Samples were mounted on aluminum SEM stubs using carbon tabs before sputter coating with gold/palladium without preliminary drying step.

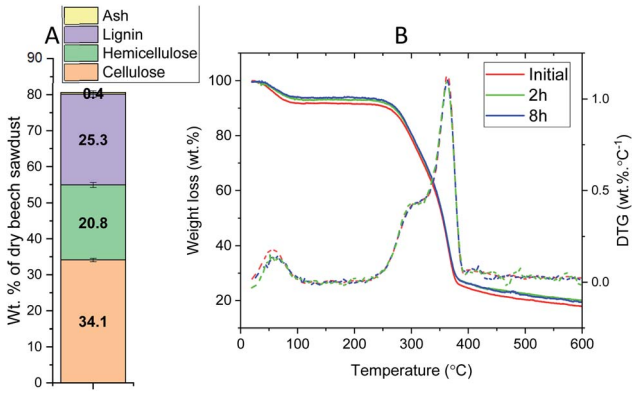

Fig. 2 (A) Biomass compositional analysis of the initial beech sawdust, (B) thermal gravimetric analysis of initial and coated beech sawdusts [1% graphite coated, 2 and 8 h ball milling, 250–500 μm].

Results and discussion

Characterisation of the initial and graphite coated beech sawdust

The beech sawdust was selected for the study due to its high contents of cellulose and hemicelluloses, which had been previously reported to favour the production of syngas (H_2, CO).[3] As illustrated in Fig. 2A, the beech sawdust contained 34 wt% of cellulose, 21 wt% of hemicelluloses and 25 wt% of acid-insoluble lignin (Klason lignin). The sawdust also possesses a very low ash content which could be indicative of its low microwave absorbance properties.

As illustrated in Fig. 2B, the thermal gravimetric analysis of the 1 wt% graphite coated sawdust (2 h and 8 h ball milling) with the initial beech sawdust showed that the hemicelluloses, cellulose and lignin decompositions were unaffected by the ball milling procedure and the presence of graphite coating. Identical thermal decomposition profiles for both sawdusts showed that the coating procedure using low rotation ball milling (120 rpm) did not alter the thermal properties of the coated beech sawdust. Previous work reported that ball milling of wood sawdust drastically modified its thermal properties by shifting hemicellulose, cellulose thermal degradation toward lower temperature.[32,33] Other previous work reported that even if cellulose crystallinity decreased with ball milling duration, the presence of graphite reduced the decrystallization due to the lubricant action.[29] In the present work, the presence of graphite and the low rotation speed (120 rpm) could explain the limited structural alteration of the wood cell wall. Indeed, the gentle ball milling was used for mechanical coating instead of sawdust powdering. As illustrated in Fig. S1,† particle size of the sawdust was affected by the ball milling duration but less than 6 wt% of fine particles (<75 μm) was produced after 8 h of ball milling. On the other hand, Table 1 shows that ball milling in presence of graphite increased the density of the sawdust from 236 to 413 kg m^{-3}. In absence of graphite, sawdust bulk density only increased to 294 kg m^{-3} after 2 h ball milling. A small loading of graphite showed positive effect on the coated sawdust density with 386 kg m^{-3} for 0.25 wt% and up to 413 kg m^{-3} for 1 wt% of graphite.

Starting from different sawdust particle sizes (75–250, 250–500 and 500–1000 μm), no effect was observed on the density of

Table 1 Density and electrical conductivity of uncoated and graphite coated beech sawdust as function of the initial particle size, graphite loading, ball milling duration and post-ball milling particle size

Initial particle size (μm)	Graphite loading (wt%)	Ball milling duration (h)	Post-ball milling particle size (μm)	Density (kg m^{-3})	Electrical conductivity (mS m^{-1})
75–250	n.a.	n.a.	n.a.	253	<0.003
250–500	n.a.	n.a.	n.a.	238	<0.003
500–1000	n.a.	n.a.	n.a.	236	<0.003
500–1000	0	2	75–1000	294	<0.003
500–1000	0.25	2	75–1000	386	<0.003
500–1000	0.25	4	250–500	410	0.75 (0.09)
500–1000	0.5	2	75–1000	402	3.0 (0.4)[b]
500–1000	0.75	2	75–1000	408	6.2 (0.7)
500–1000	1	2	75–1000	413	15.7 (1.4)
500–1000	1.25	2	75–1000	403	32.1 (3.1)
500–1000	1.5	2	75–1000	412	37.7 (1.1)
75–250	0.75	2	<250	403	<0.003
250–500	0.75	2	<500	406	0.14 (0.03)
500–1000	0.75	2	<1000	408	5.4 (0.6)
500–1000	1	1	250–500	382	0.2 (0.1)
500–1000	1	2	250–500	402	12.8 (1.8)
500–1000	1	4	250–500	416	75.0 (3.1)
500–1000	1	6	250–500	402	81.0 (1.8)
500–1000	1	8	250–500	376	80.0 (5.3)
500–1000	1	2	75–250	360	20.3 (1.9)
500–1000	1	2	500–1000	389	2.9 (0.1)
250–500[a]	5	n.a	n.a.	248	<0.003
250–500[a]	10	n.a.	n.a.	259	34 (68)

[a] Mixing of graphite with beech sawdust. [b] Standard deviation measured from 5 replicates.

the 0.75% coated materials as all three bulk densities were ranged from 403 to 408 kg m^{-3}. This suggests that the particle size (lower than 1 mm) has a low impact on the bulk density of the materials. It has been previously demonstrated that the increase of the bulk density improved the pyrolysis of cellulose.[34] Another study reported that the bulk density was not only a function of particle size distributions but also particle morphology where needle shape particles provided higher bulk density than spherical shape.[35] It is suggested here that the bulk density increase could be attributed to the flattening of the sawdust. As illustrated in Fig. S2,† the graphite coated sawdust particle exhibits a flatter and smoother surface than when the sawdust was ball milled in absence of graphite. This could explain the increase of the bulk density and is supported by previous work on exfoliation of graphite using cellulose. It was reported that the presence of graphite prevented the size reduction leading to larger particle with smooth surface attributed to the graphene stacking.[29] This phenomenon was attributed to the presence of graphite acting as a lubricant during the ball milling step. From 1 to 8 h ball milling, the results showed that the ball milling duration has little effect on the densification of the samples (250–500 μm post-ball milled particle size) with higher density reached after 4 h ball milling. Interestingly, the density slightly decreased to 376 kg m^{-3} after 8 h ball milling suggesting than prolonged ball milling have adverse effect on the densification of the coated sawdust.

Electrical conductivity of the graphite coated beech sawdust

The graphite is well known to provide electrical conductivity to mixed composites with electrical percolation threshold lower than 1 wt% for polysaccharide such as carboxymethylcellulose.[29] As illustrated in Table 1, the electrical conductivity of the graphite coated particle has been measured in order to link this parameter to the efficiency of the pyrolysis. In absence of conductivity, the value was lower than the detection threshold (0.003 mS m^{-1}). As illustrated in Fig. 3A, the electrical conductivity of the coated graphite increased from 3 to 38 mS m^{-1} with the increase of the graphite loading from 0.5 to 1.5 wt%, following a S-shape profile suggesting that higher graphite loading should not have a significant impact on the conductivity. As illustrated in Fig. 3B, the ball milling duration also increased the conductivity from 0.2 to 75 mS m^{-1} when the graphite coating time increased from 1 h to 4 h. Higher conductivity could be attributed to the exfoliation of the graphite, allowing more efficient graphite coverage of the particle. This could be visually notified by the darkening of the coated particle (see Fig. S3†). However, no increase of the conductivity was observed from 4 h to 8 h ball milling suggesting that the coating was completed after 4 h ball milling.

In term of initial sawdust particle size, 0.75 wt% coated sawdust shows no electrical conductivity for initial particle size ranged from 75–250 μm. Medium range initial particle size (250–500 μm) gave low conductivity with 0.14 mS m^{-1} while the conductivity of the larger particle size (500–1000 μm) was 5.4 mS m^{-1}. When the sieving was performed after graphite coating, the conductivity showed a different profile where 1 wt% coated sawdust with small particle size (75–250 μm) exhibited higher electrical conductivity (20.3 mS m^{-1}) than larger particle size.

Microwave activation of the graphite coated sawdust

During the microwave pyrolysis, the evolution of the heating rate confirms the behaviour of different coated samples. Fig. 4 and S4† show that the increase of microwave power (A), graphite loading (B), ball milling duration (C) and initial particle size (D) improved the temperature profile of the beech sawdust. As illustrated in Fig. 4A, the heating rate can be divided in three sections with first the water playing important role in the microwave absorbance of the samples up to 100 °C, followed with a phase of constant heating rate from 110 °C to 180 °C and finally sharp increase of the heating rate due to clarification process. In most cases, the heating rate reached its highest value at 300 °C suggesting that the produced char is better microwave absorber than the initial coated sample.

In term of graphite loading, Fig. 4B shows a small increase of susceptor from 0.25 to 0.5 wt% was enough to provide the microwave absorbance necessary for efficient pyrolysis/

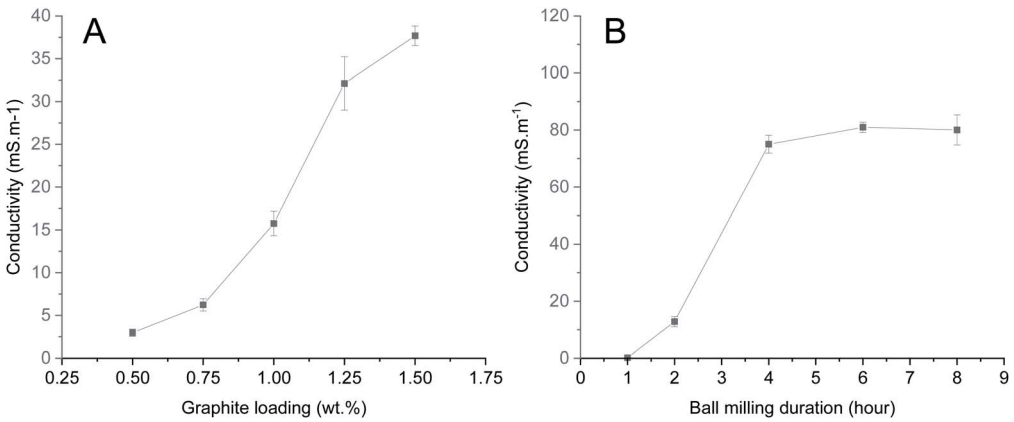

Fig. 3 Electrical conductivity properties of the graphite coated sawdust as function of the graphite loading (A) or ball milling duration (B) [(A) 2 h ball milling of initial particle size (500–1000 μm), (B) 1 wt% graphite coated of initial particle size (500–1000 μm) (selected particle size of 250–500 μm)].

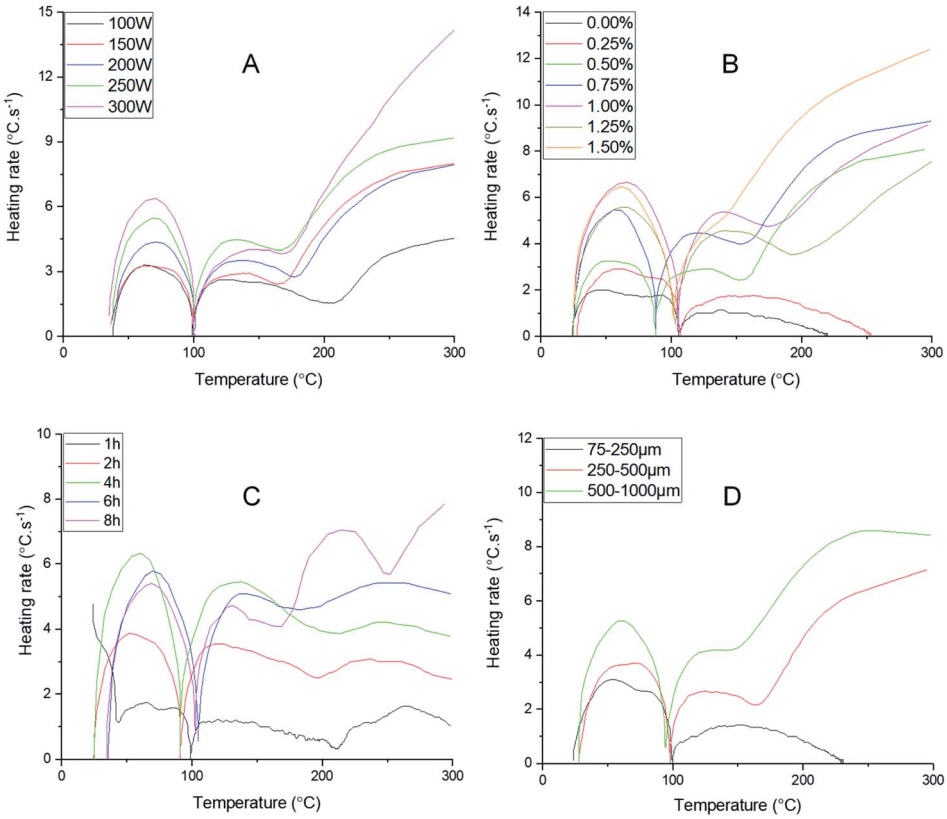

Fig. 4 Heating rate of the coated beech sawdust pyrolysis as function of the MW power (A), graphite loading (B), ball milling duration (C) and initial particle size (D) [(A) 0.5 wt% graphite coated samples (500–1000 μm), 2 h ball milling; (B) graphite coated samples (500–1000 μm), 2 h ball milling, 150 W; (C) 1 wt% graphite coated (selected particle size of 250–500 μm), 100 W; (D) 0.75 wt% graphite coated samples, 2 h ball milling, 200 W].

cracking. As illustrated in Fig. 4C, the heating rate shows that 1 h ball milling time of the 1 wt% coated samples gave heating rate around 1 °C s^{-1} at 100 W with little evolution over the temperature. This low microwave absorbance of the coated samples after 1 h ball milling already provided moderate heating rate required for pyrolysis/cracking. The increase of the ball milling time produced samples (selected particle size 250–500 μm) with higher microwave absorbance which was corroborated with the higher electrical conductivity of the samples (see Table 1). Nevertheless, Fig. S4C† shows that ball milling duration longer than 4 h has little impact on the pyrolysis temperature profile of 1 wt% graphite coated sawdust which also corroborated with the unchanged electrical conductivity (see Table 1 and Fig. 3B). When comparing the heating rate profiles as function of the initial sawdust particle size, the small particle size (75–250 μm) did not provide the microwave absorbance properties required for efficient pyrolysis. Medium and large particle size (250–500 μm and 500–1000 μm) both show higher ability to absorb microwave radiation leading to efficient pyrolysis.

Impact of the sample preparation on the pyrolysis products distribution

The graphite coated beech sawdusts were submitted to microwave-assisted thermolysis. The efficiency of the thermolysis was investigated by changing parameters such as graphite loading, microwave power, ball milling duration and sawdust particle size. Fig. 5 shows the percentage fractions of solid residues, liquids and gases obtained after the microwave-assisted pyrolysis of the beech sawdust.

Effect of the graphite coating. As illustrated in Fig. S1A,† the particle size distributions of the beech sawdust after 2 h ball milling were identical regardless of the graphite loading. After 2 h ball milling, 250–500 μm size fraction corresponded for nearly 60 wt% of the sawdust with initial particle size of 500–1000 μm. The graphite loading study revealed that in the absence of graphite (0 wt%), no pyrolysis of the beech sawdust occurred (Fig. 5A). When beech sawdust was coated with 0.25 wt% of graphite, the yield of solid residue dropped from 70.0 wt% to 47.6 wt% and 13.6 wt% of oil was produced but the gas yield remained low. At 0.5 wt% of graphite, the gasification of the sawdust increased from 7.3 (at 0.25 wt%) to 20.7 wt%. Results show that further increase of the graphite loading has lower effect on the yield of the solid, liquid and gas fractions. Densification of the biomass could not be the only explanation of the better suitability as the 0.25 wt% coated sawdust already exhibited similar bulk density to 0.5 wt% coated sawdust (see Table 1). However, the electrical conductivity of the coated sawdust could be the factor that trigger the pyrolysis. As illustrated in Table 1, while 0.25 wt% coated sawdust showed no

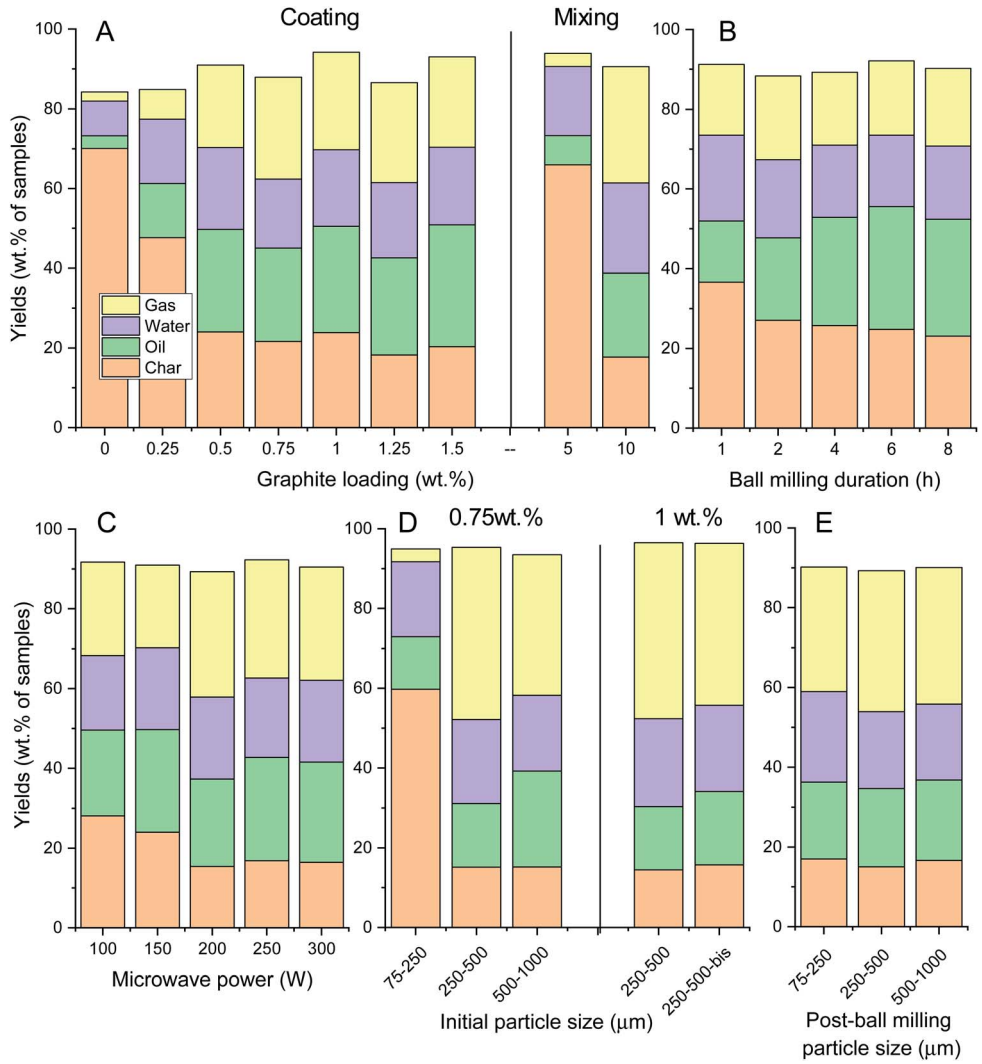

Fig. 5 Percentage of solid residue, water, oil and gases as a function of the sample preparation and microwave conditions (on the wet basis, graphite content was subtracted from the residue) [(A) for coated samples, particle size of 500–1000 μm, 2 h ball milling and 150 W; for graphite mixed sawdust, particle size of 250–500 μm, 200 W; (B) 1 wt% graphite, 250–500 μm selected particle size, 100 W; (C) 0.5 wt%, initial particle of 500–1000 μm, 2 h ball milling, (D) 0.75 or 1 wt% graphite coating, 2 h ball milling, 200 W; (E) initial particle size, 500–1000 μm, 1 wt% graphite, 2 h ball milling, 200 W].

electrical conductivity after 2 h ball milling, 0.5 wt% exhibited an electrical conductivity of 3.0 mS m^{-1}.

As illustrated in Fig. 5A, the uncoated samples with 250–500 μm as the selected particle size mixed with 5 wt% graphite did not provide the conditions required for pyrolysis/cracking In contrast, 10 wt% graphite loading provided the microwave absorbance necessary for efficient pyrolysis/cracking of the beech sawdust. With similar conversion of the biomass to bio-oil and bio-gas, graphite catalytic coating of the beech sawdust using mechano-assisted procedure allows the reduction the need for microwave susceptor by a factor 10.

Effect of the ball milling duration. In order to avoid any particle size reduction effect due to ball milling time (see Fig. S1B†), the pyrolysis was performed on the selected particle size (250–500 μm) of the 1 wt% graphite coated sawdust. The effect of the duration of the ball milling was reported in Fig. 5B. Low microwave power (100 W) was selected in order to highlight any step improvement of the graphite coating. As illustrated in Fig. 5B, the yields of solid residue decreased from 36.6 wt% to 23.1 wt% when the ball milling duration increased from 1 to 8 h. As low as 1 h ball milling time already allowed pyrolysis and gasification to occur with 15.3 wt% and 17.6 wt% yields for bio-oil and bio-gas, respectively. The increase of the ball milling time to 2 h increased the bio-oil to 20.6 wt% and the bio-gas to 21.0 wt% while decreasing the residue to 27.1 wt%. Further increase of the ball milling duration decreased the solid residue and surprisingly increased the bio-oil up to 30.8 wt% for 6 h ball milling while the bio-gas yield was little affected. In other words, the increase of the ball milling time from 2 to 8 h had little effect on the pyrolysis/cracking efficiency of the sawdust.

Effect of the microwave power. The increase of the microwave power was expected to affect the products fraction

distributions. As illustrated in Fig. 5C, low MW power (100 W) already provided pyrolysis conditions with 21.5 wt% of bio-oil and 23.4 wt% of gases for 28.1 wt% of solid residue. This could be confirmed by the heating rate of samples microwaved at 100 W (see Fig. 4A). Increase of the power to 200 W increased the gas fraction to 31.4 wt% while the mass of solid residue was reduced to 15.4 wt%. Higher MW power showed no effect on the gasification efficiency as gas yield remained unchanged for 250 and 300 W.

Effect of the initial beech particle size. Three sawdust samples with different particle sizes (75–250, 250–500 and 500–1000 μm) were coated with 0.75 wt% of graphite for 2 h and pyrolysed at 200 W. Fig. 5D shows that the initial particle size of the sawdust has more impact on the products distribution than the graphite loading, microwave power and ball milling duration. When small particles size (75–250 μm) were used for the coating stage, high yield of solid residue combined with low yield of bio-oil and absence of biogas revealed that sample preparation did not provide the microwave absorbance properties required for pyrolysis/cracking. On the other hand, the use of the largest initial particles size (500–1000 μm) resulted in efficient pyrolysis/cracking. The yield of solid residue dropped to 15.2 wt% while the bio-oil increased to 24.0 wt% and the biogas to 35.2 wt%. More interesting was the medium range particle size (250–500 μm) providing the highest gasification yield (43.2 wt%) to the detriment of bio-oil (16.0 wt%). Without considering the water unavoidably generated from pyrolysis of the sawdust, the selectivity toward the gas fraction was close to 60 wt%. The 2 h ball mill coating of the selected sawdust particles (250–500 μm) with 0.75 wt% of graphite provided excellent samples properties for efficient pyrolysis. In the case of small particle size (75–250 μm), the large surface area of samples led to discontinued graphite coating, explaining its low microwave absorbance capacity and the absence of pyrolysis. This sample did not show electrical conductivity. In the case of the large initial particle size (500–1000 μm), the graphite coating was easily completed (electrical conductivity of 5.4 mS m^{-1}) after 2 h of ball milling. However, the large particle size led to a greater temperature gradient between the surface (graphite coating) and the inside of the particle, which could explain the higher amount of oil being produced. The medium range particle size (250–500 μm) provided the best samples with both high graphite coating and quick heat transfer from the outer to the inner part of the particle. To confirm the good performance of the medium range sample size, 1 wt% of graphite coated sawdust (initial particle size 250–500 μm) was gasified at 200 W to produce comparable products distribution with on average 15, 17 and 42 wt% of biochar, bio-oil and bio-gas respectively (see Fig. 5D).

Effect of the post-ball milling particle size. Initial particle sawdust sizes have been shown to impact on the efficiency of pyrolysis/cracking especially due to the lack of graphite covering. In order to check the impact of the particle size after ball milling, the 1 wt% coated samples (initial particle size ranged from 500 to 1000 μm) were sieved to provide three particles size (75–250, 250–500 and 500–1000 μm). The results show that the post-ball milling particle sizes have little effect on the gasification efficiency with gas yields ranged from 31.2 to 35.3 wt% (see Fig. 5E). This suggested that the sawdust particle size did not impact the gasification yield if efficient graphite coating was produced and sample electrical conductivity was observed.

Effect of the sample electrical conductivity. A trend could be drawn between electrical conductivity of the coated sawdust and thermolysis efficiency. The absence of biomass gasification could be attributed to the electrical conductivity of the samples below 0.003 mS m^{-1} (detection threshold). On the other hand, no increase of the gas yields was observed for 0.5 to 1.5 wt% coated sawdust (see Table 2) while the conductivity greatly improved from 3 to 38 mS m^{-1}. For the impact of the ball milling duration, the increase of the conductivity from 0.2 to 81 mS m^{-1} for 1 h and 6 h ball-milled samples had low impact on the gas yield. With a conductivity as low as 0.13 mS m^{-1} (see Table 1), the pyrolysis/cracking of the 0.75 wt% coated sawdust with initial particle size ranged from 250 to 500 μm gave one of the highest gas yields suggesting that only low conductivity are required for efficient gasification. It could be postulated that the electrical conductivity provides an OFF/ON rather than a gradual response for the efficiency of the pyrolysis/cracking. Below the conductivity threshold, the biomass could not be gasified while above that value, higher conductivity did not contribute to higher gas yields. In the case of wood sawdust, the measurement of the sample's conductivity prior microwave assisted pyrolysis could be a useful tool to predict the efficiency of the lignocellulosic biomass cracking. To provide conductive sample, the results demonstrates that the initial particle size of the sawdust, graphite loading, and ball mill duration all affected the ability to efficiently coat the wood particle and subsequently producing conductive sawdust samples.

Pyrolysis gases compositions as a function of the experimental conditions

As illustrated in Table 2, the composition of the gas showed that carbon monoxide accounts for up to 50 vol% of the total gas. Hydrogen was the second most abundant gas with up to 27 vol% of the total gases. In most of the conditions, the combined relative volume of H_2 and CO was above 75 vol%. The gas composition is comparable to previous work on the microwave assisted-gasification of pine sawdust where 45, 25, 12 and 12 vol% of CO, H_2, CO_2 and CH_4 were produced at 600 °C.[19] This work also highlighted the impact of the temperature on the relative ratio of non-condensable gases where less than 17 vol% of H_2 was produced for MAP temperature of 400 °C. This suggests that while the bulk temperature did not excess 300 °C, localised hotspot must be far in excess of these temperature. It is worth noting that gas was already produced while the bulk temperature was lower than 150 °C. This observation was previously explained by micro-plasma formation due to the presence of graphitic materials.[36,37]

Based on the microwave power input, relative volume of CO_2 decreased with the increase of the microwave power from 100 to 200 W while the CO and C_2 gases increased. The high amount of CO_2 at low power input (100 W) suggest the decarboxylation of

Table 2 Quantitative analysis of the pyrolysis gas for various sawdust samples preparation and microwave conditions

	Total gas volume (mL g^{-1} of dry sawdust)	Relative vol%							Vol ratio	Wt% (g/100 g of dry sawdust)			
		H_2	CO	CH_4	CO_2	C_2H_2	C_2H_4	C_2H_6	CO/H_2	H_2	CO	CH_4	CO_2
Microwave power (0.5 wt%, 500–1000 μm, 2 h ball milling)													
100 W	251	23.7	44.8	9.8	18.8	0	2.3	0.5	1.9	0.5	13.1	1.6	8.6
150 W	257	23.4	46.8	9.4	16.8	0.3	2.7	0.5	2	0.5	14	1.6	7.9
200 W	358	25.4	48.7	8.9	12.4	1	3.3	0.2	1.9	0.4	20.3	2.1	8.1
250 W	342	25.3	49.9	8.5	12	1.3	2.8	0.3	2	0.7	19.8	1.9	7.5
300 W	320	23.7	49.6	9	12.9	1.2	3.2	0.4	2.1	0.6	18.4	1.9	7.5
Ball milling duration (1 wt%, 250–500 μm, 100 W)													
1 h	182	23.1	40.9	10	23.6	0	1.8	0.6	1.8	0.3	8.6	1.2	7.8
2 h	220	22.6	44.3	10	20.3	0	2.3	0.6	2	0.4	11.3	1.5	8.2
4 h	189	21.6	45.5	9.6	20.5	0	2.2	0.6	2.1	0.3	10	1.2	7.1
6 h	191	21.1	45.9	9.7	21	0	1.8	0.6	2.2	0.3	10.2	1.2	7.3
8 h	204	21.5	47.4	9.7	18.6	0	2.2	0.5	2.2	0.4	11.2	1.3	6.9
Graphite loading on coated samples (500–1000 μm, 2 h ball milling, 150 W)													
0%	14	0	42.4	0	57.6	0	0	0		0.0	0.7	0	1.5
0.25%	52	1.2	46.5	3.7	47.9	0	0.3	0.4	38.8	0.0	2.8	0.1	4.5
0.50%	257	23.4	46.8	9.4	16.8	0.3	2.7	0.5	2	0.5	14	1.6	7.9
0.75%	279	23.3	48.4	9.2	15.8	0	2.8	0.5	2.1	0.5	15.7	1.7	8
1%	265	22.5	47.7	9.6	16.2	0.5	3	0.5	2.1	0.5	14.7	1.7	7.9
1.25%	274	23.9	46.4	9.5	16.3	0.5	3	0.4	1.9	0.5	14.7	1.7	8.1
1.50%	248	23.6	47.7	9.2	15.8	0.4	2.8	0.4	2	0.5	13.7	1.5	7.2
Graphite loading on uncoated samples (250–500 μm, 200 W)													
5%	24	0	41.9	0	58.1	0	0	0		0.0	1.1	0	2.5
10%	357	26.2	50.1	8.8	11	1.1	2.6	0.3	1.9	0.8	20.8	2.1	7.1
Initial particle size (0.75 or 1 wt%, 2 h ball milling, 200 W)													
75–250 μm/0.75	23	0	40.2	0	59.8	0	0	0		0.0	1.1	0	2.5
250–500 μm/0.75	515	24.4	49.7	9.7	11.2	1.5	3.1	0.3	2	1.0	29.7	3.3	10.6
500–1000 μm/0.75	428	26.9	48.2	8.5	11.8	1.2	2.9	0.3	1.8	1.0	24	2.4	9.3
Post-ball milling particle size (500–1000 μm, 1 wt%, 2 h ball milling, 200 W)													
75 to 250 μm	388	28.4	49.6	7.8	10.5	1.0	2.4	0.2	1.7	0.9	22.3	2.0	7.4
250 to 500 μm	422	25.4	49.3	9.0	11.9	0.9	3.1	0.4	1.9	0.9	24.1	2.5	9.2
500 to 1000 μm	421	27.9	49.4	7.8	11.0	1.2	2.3	0.3	1.8	1.0	24.2	2.2	8.5

the biomass required less energy than CO and H_2 production which is in accordance with previous work on microwave-assisted pyrolysis of pine sawdust.[19] The microwave power has a low impact on the relative amount of hydrogen and methane. At 0.5 wt% graphite coating, maximum gas volume (358 mL g^{-1}) was reached for microwave power of 200 W. Except for 1 h duration where the CO was the lowest, the ball milling time does not affect the composition of the gases. From 0.5 wt% to 1.5 wt% graphite coating, the constant gas volumes and compositions suggest that there is no effect of the amount of graphite coating on the gas yield when the samples were irradiated at 150 W. This highlights that catalytic amount of graphite was enough to provide sufficient coating and excess of graphite was unnecessary. In term of mass yield, up to 30 wt% of the sawdust was converted to carbon monoxide when initial particle sizes (250–500 μm) were coated with 0.75 wt% of graphite and gasified using 200 W microwave power. When the pyrolysis was performed on 1 wt% coated sawdust with initial particle sizes from 250 to 500 μm, similar amount of gases (496 and 522 mL g^{-1}) were produced from two consecutive runs confirming the optimal conditions for efficient gasification. In term of CO/H_2 ratio, the Table 2 shows that the values fluctuated between 1.7 to 2.2 when the samples gasification happened. However, it was previously reported that each individual components of the biomass (lignin, cellulose and hemicelluloses) contributed differently in the production of gases.[38,39] Even if the amount of gas increased from 180 to 522 mL g^{-1} of sawdust, the constant CO/H_2 ratio suggested a constant relative amount of cellulose, hemicelluloses and lignin were gasified regardless the conditions applied. As consequence, the increase of gas yields should be attributed to a greater proportion of biomass due to more volumetric and fast heating rate rather than specific activation of components within the biomass. Huang *et al.* used the biomass component analysis to predictive the gas yield and composition.[38] Based on his predictive equations, the amount of hydrogen, carbon monoxide, carbon dioxide and methane should be respectively 0.6, 21.5, 7.1 and 1.6 wt% of the dry sawdust. Those predictive

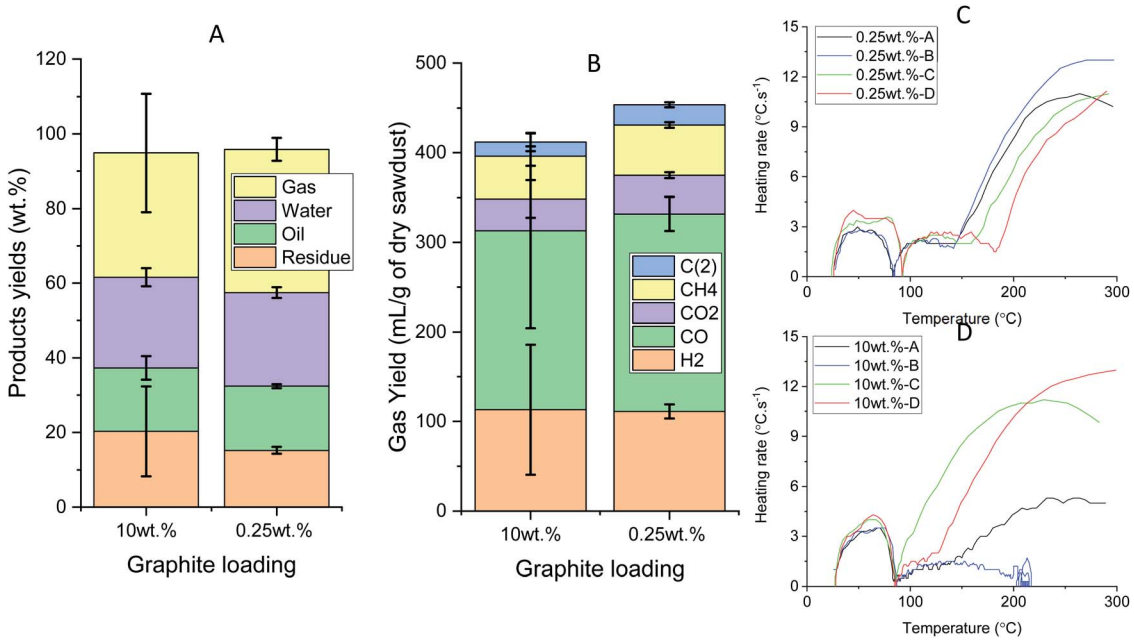

Fig. 6 Experimental reproducibility of the microwave assisted pyrolysis of 10 wt% graphite loaded against 0.25 wt% graphite coated sawdusts [products yields distributions (A), gas composition (B) and heating rate profiles (C and D) for 10 wt% mixed or 0.25 wt% coated sawdust, selected particle size from 250 to 500 μm, 200 W].

values are 27 and 45 wt% lower than the yields of CO–CO_2 and H_2–CH_4 obtained in our best conditions (515 mL g^{-1}).

Reproducibility of the microwave-assisted pyrolysis of graphite loading beech sawdust

In the case of uncoated sawdust, a 10 wt% graphite loading sample provided inconsistent conductivity from several measurements with 34 ± 68 mS m^{-1} (see Table 1). This highlighted that simple mechanical mixing of graphite within the sawdust particle provided inhomogeneous graphite distribution, which led to poor reproducibility of the thermolysis results.

As illustrated in Fig. 6A, five successive pyrolysis runs of 10 wt% graphite loaded beech sawdust generated on average 33 ± 16 wt% of gas with value ranging from 9.0 to 49.1 wt%. The inconsistency of the gas and solid yields was exacerbated by the failure to provide pyrolysis/cracking condition for one of the repetitions. On the other hand, the catalytic graphite coating was able to provide excellent reproducibility. As illustrated in Fig. 6B, four consecutive runs of the 0.25 wt% graphite coated sawdust (particle ranged from 250 to 500 mm) generated consistent results with 38 ± 3 wt% of gas. The higher reproducibility of the graphite coated sample compared to the mixed sample can also be seen from the higher constituency of the pyrolysis heating rate (Fig. 6C and D). The 10 wt% mixed sawdust provided poor heating rate reproducibility (Fig. 6D) certainly due to the inhomogeneous distribution of the graphite within the samples. On the other hand, the advantage of the coating is the homogeneous coverage of the graphite on the surface of the particles which provide better distribution of the heat to the sawdust particle. Moreover, the coated sawdust particle could act as a support for the graphite homogeneously introduced in the reactor. On the top of being more efficient, the mechano-assisted graphite coating of the beech sawdust could offer several advantages in scale-up procedure toward continuous microwave thermolysis processes.

Conclusion

Compared to simple susceptor mixing with the biomass, graphite coating of the sawdust provides more effective pyrolysis/cracking with more than 20 times less graphite loading, requiring only catalytic amount of the susceptor. Amongst all parameters, the initial particle size of the sawdust had the highest impact on the gas yield. A combination between efficient graphite coating and low temperature gradient between the inner and outer part of the particle could explain the higher gas yield for the medium range initial particle size (250–500 μm). In this optimal condition, 515 mL of gases per gram of dry biomass were produced with CO yield as high as 30 wt% of the biomass. The electrical conductivity of the coated sawdust was a good indicator of how the wood sample will gasify with as low as 0.14 mS m^{-1} of conductivity required for high syngas production. This indicator could be easily implemented on large scale production as in-line pretesting before the microwave pyrolysis. By improving the microwave absorbance properties of the woody biomass, the catalytic graphite coating of the beech sawdust provides practical solution for continuous pyrolysis, reducing the microwave energy consumption while improving syngas production.

Conflicts of interest

There are no conflicts to declare.

Acknowledgements

This work is financially supported by the Industrial Biotechnology Catalyst (Innovate UK, BBSRC, EPSRC) to support the translation, development and commercialization of innovative industrial Biotechnology processes (EP/N013522/1). The authors thank Dr Hannah Bries, Dr Richard Gammons and Dr Clare Steele-King for expert technical assistance.

Notes and references

1 T. P. Vispute, H. Zhang, A. Sanna, R. Xiao and G. W. Huber, *Science*, 2010, **330**, 1222–1227.
2 J. H. Clark, *J. Chem. Technol. Biotechnol.*, 2007, **82**, 603–609.
3 V. S. Sikarwar, M. Zhao, P. Clough, J. Yao, X. Zhong, M. Z. Memon, N. Shah, E. J. Anthony and P. S. Fennell, *Energy Environ. Sci.*, 2016, **9**, 2939–2977.
4 X. Zhao, H. Zhou, V. S. Sikarwar, M. Zhao, A.-H. A. Park, P. S. Fennell, L. Shen and L.-S. Fan, *Energy Environ. Sci.*, 2017, **10**, 1885–1910.
5 R. Luque, C. S. K. Lin, K. Wilson and J. Clark, *Handbook of Biofuels Production: Processes and Technologies*, 2nd edn, 2016.
6 J. Sherwood, M. De Bruyn, A. Constantinou, L. Moity, C. R. McElroy, T. J. Farmer, T. Duncan, W. Raverty, A. J. Hunt and J. H. Clark, *Chem. Commun.*, 2014, **50**, 9650–9652.
7 S. Su, R. Kopitzky, S. Tolga and S. Kabasci, *Polymers*, 2019, **11**, 1193.
8 M. Rüegsegger and M. Kast, *Lessons Learned about Thermal Biomass Gasification*, IEA Bioenergy, 2018.
9 M. De bruyn, J. Fan, V. L. Budarin, D. J. Macquarrie, L. D. Gomez, R. Simister, T. J. Farmer, W. D. Raverty, S. J. McQueen-Mason and J. H. Clark, *Energy Environ. Sci.*, 2016, **9**, 2571–2574.
10 S. Tsubaki, Y. Nakasako, N. Ohara, M. Nishioka, S. Fujii and Y. Wada, *Green Chem.*, 2020, **22**, 342–351.
11 Y.-F. Huang, P.-T. Chiueh and S.-L. Lo, *Sustainable Environ. Res.*, 2016, **26**, 103–109.
12 S. Y. Foong, R. K. Liew, Y. Yang, Y. W. Cheng, P. N. Y. Yek, W. A. Wan Mahari, X. Y. Lee, C. S. Han, D.-V. N. Vo, Q. Van Le, M. Aghbashlo, M. Tabatabaei, C. Sonne, W. Peng and S. S. Lam, *Chem. Eng. J.*, 2020, **389**, 124401.
13 R. Luque, J. A. Menéndez, A. Arenillas and J. Cot, *Energy Environ. Sci.*, 2012, **5**, 5481–5488.
14 B. F. Fernandez, *Renew. Energy Focus*, 2015, **16**, 156–159.
15 M. J. Gronnow, V. L. Budarin, J. Fan, P. S. Shuttleworth, D. J. MacQuarrie and J. H. Clark, *Microwave pyrolysis of biomass Conference Proceeding: Technical Proceedings of the CTSI Clean Technology and Sustainable Industries Conference and Expo*, Boston, MA, United States, 2011, pp. 679–682.
16 T. Li, J. Remon, P. S. Shuttleworth, Z. Jiang, J. Fan, J. H. Clark and V. L. Budarin, *Energy Convers. Manage.*, 2017, **144**, 104–113.
17 M. Miura, H. Kaga, A. Sakurai, T. Kakuchi and K. Takahashi, *J. Anal. Appl. Pyrolysis*, 2004, **71**, 187–199.
18 C. Ellison, M. McKeown, S. Trabelsi and D. Boldor, *Energies*, 2017, **10**, 502.
19 X.-H. Wang, H.-P. Chen, X.-J. Ding, H.-P. Yang, S.-H. Zhang and Y.-Q. Shen, *BioResources*, 2009, **4**, 946–959.
20 S. Zhang, Q. Dong, L. Zhang and Y. Xiong, *Bioresour. Technol.*, 2015, **191**, 17–23.
21 Q. Bu, H. Lei, S. Ren, L. Wang, J. Holladay, Q. Zhang, J. Tang and R. Ruan, *Bioresour. Technol.*, 2011, **102**, 7004–7007.
22 Q. Xie, F. C. Borges, Y. Cheng, Y. Wan, Y. Li, X. Lin, Y. Liu, F. Hussain, P. Chen and R. Ruan, *Bioresour. Technol.*, 2014, **156**, 291–296.
23 S. Liu, Y. Zhang, L. Fan, N. Zhou, G. Tian, X. Zhu, Y. Cheng, Y. Wang, Y. Liu, P. Chen and R. Ruan, *Fuel*, 2017, **196**, 261–268.
24 P. Lahijani, M. Mohammadi, Z. A. Zainal and A. R. Mohamed, *Thermochim. Acta*, 2015, **604**, 61–66.
25 N. Xiao, H. Luo, W. Wei, Z. Tang, B. Hu, L. Kong and Y. Sun, *J. Anal. Appl. Pyrolysis*, 2015, **112**, 173–179.
26 W. Liu, H. Jiang, X. Zhang, Y. Zhao, S. Sun and J. Qiao, *J. Mater. Chem. A*, 2019, **7**, 27236–27240.
27 Z. Du, Y. Li, X. Wang, Y. Wan, Q. Chen, C. Wang, X. Lin, Y. Liu, P. Chen and R. Ruan, *Bioresour. Technol.*, 2011, **102**, 4890–4896.
28 C. M. Cova and R. Luque, *BMC Chem. Eng.*, 2019, **1**, 16.
29 P. Sun, S. Kuga, M. Wu and Y. Huang, *Cellulose*, 2014, **21**, 2469–2478.
30 W. Zhao, M. Fang, F. Wu, H. Wu, L. Wang and G. Chen, *J. Mater. Chem.*, 2010, **20**, 5817–5819.
31 Y. Hernandez, V. Nicolosi, M. Lotya, F. M. Blighe, Z. Sun, S. De, I. T. McGovern, B. Holland, M. Byrne, Y. K. Gun'Ko, J. J. Boland, P. Niraj, G. Duesberg, S. Krishnamurthy, R. Goodhue, J. Hutchison, V. Scardaci, A. C. Ferrari and J. N. Coleman, *Nat. Nanotechnol.*, 2008, **3**, 563–568.
32 A. Hideno, *BioResources*, 2016, **11**, 6309–6319.
33 C. Gong, J. Huang, C. Feng, G. Wang, L. Tabil and D. Wang, *Bioresour. Technol.*, 2016, **214**, 242–247.
34 J. Fan, P. S. Shuttleworth, M. Gronnow, S. W. Breeden, J. H. Clark, D. J. MacQuarrie and V. L. Budarin, *ACS Sustainable Chem. Eng.*, 2018, **6**, 2916–2920.
35 K. Tannous, P. S. Lam, S. Sokhansanj and J. R. Grace, *Part. Sci. Technol.*, 2013, **31**, 291–300.
36 D. V. Suriapparao, N. Pradeep and R. Vinu, *Energy Fuels*, 2015, **29**, 2571–2581.
37 J. A. Menéndez, E. J. Juárez-Pérez, E. Ruisánchez, J. M. Bermúdez and A. Arenillas, *Carbon*, 2011, **49**, 346–349.
38 Y.-F. Huang, P.-T. Chiueh, W.-H. Kuan and S.-L. Lo, *Energy*, 2015, **89**, 974–981.
39 S.-L. Lo, Y.-F. Huang, P.-T. Chiueh and W.-H. Kuan, *Energy Procedia*, 2017, **105**, 41–46.